Bulk state confinement and band folding in nanostructured surfaces

C. Didiot, V. Cherkez, B. Kierren, Y. Fagot-Revurat, and D. Malterre*
Institut Jean Lamour, UMR 7198, Nancy-Université, BP 239, F-54506 Vandœuvre-lès-Nancy, France
(Received 20 November 2009; revised manuscript received 23 January 2010; published 17 February 2010)

In the recent years, many studies showed that the surface states of noble metals can be confined in natural or artificial nanostructures on surfaces. Moreover, they can also be sensitive to periodic nanostructuration of the surfaces and can form bands with this superperiodicity. In this paper, we show by scanning tunneling spectroscopy that similar behaviors can be observed on bulk states. We present evidences of lateral confinement and "band folding" of the bulk state in Cl-based quantum corrals on Au(111) and vicinal Au(23 23 21) surfaces.

DOI: 10.1103/PhysRevB.81.075421 PACS number(s): 73.20.At, 79.60.Bm, 68.37.Ef, 72.10.Fk

I. INTRODUCTION

The response of the electron states to a localized perturbation is a well-known phenomenon, explained in the 50th by Friedel.[1] It leads to a modulation of charge and eventually spin density to screen the localized potential. The existence of a Fermi surface yields an asymptotic behavior of the charge density of states which is modulated by $\sin 2k_F r/r^d$, where k_F is the Fermi wave vector (Friedel oscillations) and d the dimensionality of the electron gas. These oscillations are essential to explain the transport and magnetic properties of impurities diluted in metals. The development of scanning tunneling microscopy (STM) and spectroscopy (STS) allows the direct observation and measurement of the oscillations of electron density at surfaces around impurities (0D defect) and step edges [one-dimensional (1D) defect].[2,3] The Friedel oscillations could play an important role in step-step interaction at a metal surface[4] or in the equilibrium distance between adatoms at low temperature.[5] They could also be used to measure the coherence length and lifetime of hot quasiparticles on metal surfaces.[6]

Surface states which are strongly localized close to the surface are very sensitive to any modification of the surface potential. Constructive interference scattering by adatoms can lead to the confinement in artificial quantum corrals obtained by atom manipulation with the STM tip.[7] A similar confinement can be obtained in nanoislands.[8–10] Such systems exhibit well-defined quantum well modes whose energies depend on shape and size of the nanostructures. In self-organized nanostructurated surfaces, the surface state can be coherently scattered to form surface band exhibiting the superperiodicity associated with periodic nanostructures. This is the case of step-edge lattices in vicinal surface,[11] surface reconstruction,[12] or self-organized nanostructures.[13]

In the last 10 years, it has been shown that bulk states can be also sensitive to localized potential at the surface. Under certain conditions on the tip apex, scattered electron density around surface defects in noble metal contains not only a surface state but also a bulk contribution. From a Fourier transform analysis of the STM image recorded with a low bias voltage, it was demonstrated that standing waves around impurities on Cu(111) and Au(111) result from both surface and bulk states whereas bulk electrons do not contribute to the screening of step edges.[14] Moreover, these bulk states imaged by STM come from the edge of the bulk Fermi-surface neck close to the L point of the Brillouin zone. Recently, oscillations of the charge density were observed on a terrace of the Ag(110) in an energy range without any surface states.[15] The authors showed that these oscillations correspond to states at the edge of the surface-projected bulk band. The predominant role of these particular states was attributed to a van Hove-like enhancement due to the bulk band curvature.

Here we report several measurements which demonstrate that bulk states exhibit electronic behaviors which are very similar with those observed with surface states. On flat and vicinal Au(111) surfaces, the STS images evidence spectral resonances of bulk states in quantum corrals and in terraces which reveal the lateral confinement of the bulk states. The perpendicular wave vector corresponding to these STS signature is found to be close to the L point of the Brillouin zone. We also show a bulk electron Bragg diffraction which reveals the superperiodicity associated with the surface nanostructuration. In all cases, the results show that the bulk states at the edge of the surface-projected band play an important role.

II. EXPERIMENTAL DETAILS

The experiments were carried out in a UHV setup composed of a molecular-beam epitaxy chamber for the elaboration and characterization of the surfaces, a STM chamber equipped with a 5 K Omicron STM, and a photoemission chamber with a high-resolution Scienta SES 200 analyzer. The samples were cleaned by several cycles of Ar^+ etching and annealing at 500 °C and it was characterized by STM and auger electron spectroscopy (AES). Halogen gas was introduced from a piezodrived leak valve at a typical pressure of 10^{-9} mbars. Exposure of few seconds (10–30 s) resulted in a Cl coverage ranging from 0.001 to 0.003 ML as measured by STM. The Au(111) and Au(23 23 21) surfaces were exposed at room temperature and further cooled down to 5 K inside the STM. The dI/dV maps were obtained from open feedback loop measurements at 5 K using the lock-in technique with a bias modulation of 10 meV at 700 Hz. The typical stabilization parameters before recording dI/dV spectra at every points of the topographic frames were $I_t = 0.5$ nA and $U_g = -1$ V.

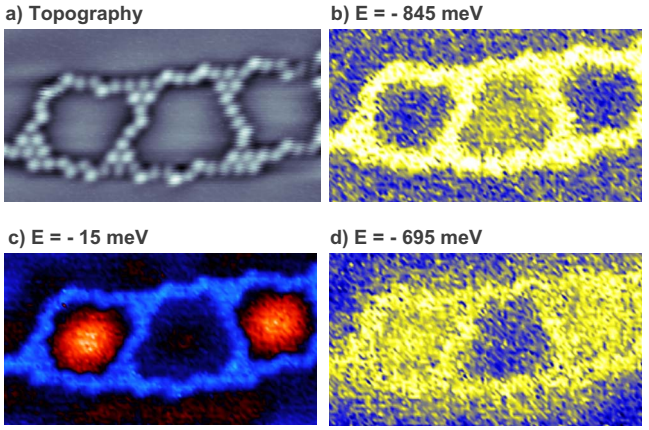

FIG. 1. (Color online) STM image (a) of three Cl rings on Au(111) grown in a fcc domain (I_t=0.5 nA and U_g=−1 V) and dI/dV maps for different voltage illustrating resonances for [(b) and (d)] bulk states and (c) surface states.

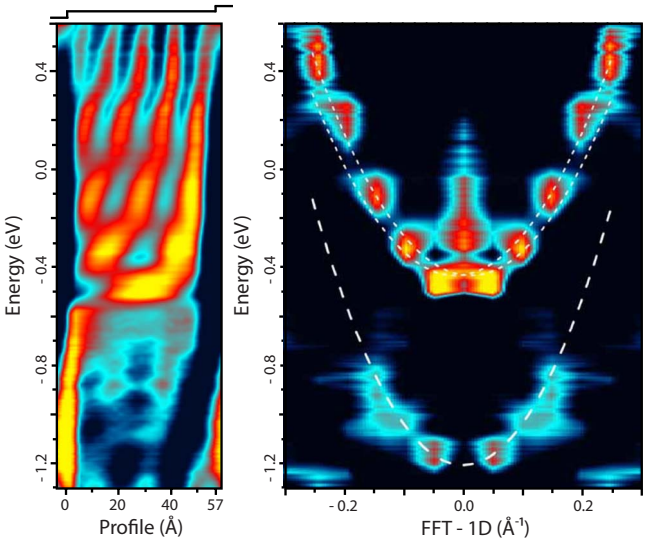

FIG. 2. (Color online) (a) dI/dV map obtained from 64 dI/dV spectra recorded on Au(23 23 21) with open back loop I_t=0.5 nA and U_g=−1.1 V. (b) 1D-Fourier transform of the dI/dV map showing the quantum well states associated with surface and bulk states. Dashed lines represent the dispersions for surface and bulk band-edge states (E_S=−0.435 eV, E_B=−1.05 eV), with their corresponding effective masses (m_S=0.26, m_B=0.19).

III. EXPERIMENTAL RESULTS AND DISCUSSION

In the low coverage regime, halogen molecules are known to dissociate on noble-metal surfaces and are adsorbed as atomiclike specie. On (111) surfaces, the adsorption site has been identified as the fcc one. For a critical coverage of 1/3 of monolayer (with respect to the substrate), a commensurate structure $(\sqrt{3}\times\sqrt{3})R30°$ can be stabilized at room temperature or lower depending on the substrate.[16] When adsorbed at room temperature on Au(111), it is also possible to obtain after cooling down to 5 K original ringlike structures for coverage much lower than 1/3 of monolayer. According to the amount of Cl atoms deposited, it is possible to obtain isolated, pair, or chains of nanorings of typical diameter about 3 nm. These rings only form inside the fcc domains of the herringbone reconstruction. In Fig. 1(a), we present a STM image showing three connected rings. These rings can be considered as quantum corrals for the surface Shockley state of the Au(111) substrate. The ring walls are one-Cl-atom thick and play the role of a large repulsive potential. Above the onset of Shockley surface state (E_S=−0.5 eV), we can evidence the different confined modes with increasing bias voltage. In Figs. 1(b) and 1(c), we report dI/dV maps for two different energies well below the onset of the surface state (E=−845 meV and E=−695 meV). They show spectral resonances, respectively, in the central and lateral rings. These resonances are very similar to the spectral signatures associated with the surface state confinement appearing at higher energy and they can be interpreted to be due to the lateral confinement of the bulk state in these nanostructures. As quantum confinement behavior is a size effect, the in-plane wave vector component of the bulk state and surface state should be equal. Both surface and bulk confined states exhibits the size effect and the smaller the ring is, the larger the confined energy is. As the two lateral corrals are slightly smaller than the central one, the ground-state resonance appears at a higher energy. These results qualitatively prove that bulk states can exhibit spectral behaviors which are very similar to the confinement of surface state in nanostructures. This is the first evidence of such effect on bulk band states in quantum corrals. One has to note that the amplitude of standing waves arising from bulk state confinement by quantum corrals is 3.5 times smaller than for the case of surface state (referred to the background level outside of the corrals). In the surface state, the increase in the LDOS in the corrals at E=−15 meV was found typically of 70% but it can be tip dependent.

In the following, we would like to show that the bulk states can also be affected by a surface superperiodicity such as, for example, in vicinal surfaces and surface reconstructions. The Shockley state in the Au(23 23 21) vicinal surface is known to be confined in the direction perpendicular to step edges and normally propagates in the parallel direction.[11] Such resonators are then one dimensional and exhibit interferences which are very similar to those observed in optics in a Fabry-Pérot interferometer.[17] In Fig. 2(a), we plot a dI/dV map as a function of energy (vertical axis) and position (horizontal axis) on a line perpendicular to step edges of the Au vicinal surface. Above $E\sim-0.5$ eV, the spectral features can be associated with the different modes of the 1D interferometer for the surface state. The asymmetry of the map reflects the asymmetry of the interferometer due to the ascending and descending steps. In the right-hand part of the figure, we plot the 1D-Fourier transform of the dI/dV map: a Fourier transform has been carried out at every line [constant energy cut of Fig. 2(a)]. This procedure gives the topology of states in reciprocal space, i.e., the momentum components of the confined states. As expected, for each mode, the dominant momenta are found on the parabolic dispersion of the surface state illustrating its nearly free-electron character. What we would like to point out is the presence of spectral intensity well below the onset of the surface state. This intensity modulation is less pronounced than for the surface state but

is clearly revealed by the Fourier transform procedure. The map of Fig. 2(b) shows that the momentum component distribution is very similar to the surface state one but is found at the edge of the surface-projected bulk band (dotted line parabolic dispersion with the bulk effective mass). As above for the confinement in quantum corrals, we interpret these spectral features by the lateral confinement of the bulk states. This is a surprising behavior because the electron dispersion in the direction perpendicular to the surface is a continuum spectrum. The well-defined energies of these laterally confined bulk states suggest that the wave vector component perpendicular to the surface is not arbitrary. Such a behavior was previously observed in a terrace of the Ag(110) surface[15] and was explained in this case by a van Hove resonance in the density of states.

How can we describe this spectral behavior of the bulk state we observed on the vicinal Au (23 23 21) surface and understand the role of the perpendicular wave vectors? Due to the 1D confinement of the surface state between two steps, there is a shift in its energy and the bottom of the lowest subband E_A (associated with the fundamental 1D-confined mode) is given by $E_A=\hbar^2k_S^2/2m_S+E_S$, where k_S is the surface wave vector perpendicular to step edges and E_S the surface state energy at the Γ point. This wave vector k_S is determined by the width of the terrace. A similar behavior is expected for the bulk state with wave vector $\vec{k}=(\vec{k}_\parallel,k_z)$ leading to a lateral confinement of the bulk states in the surface resonator. But we have to understand the well-defined energy for the STS features since the perpendicular contribution of the bulk wave vector (k_z) forms a continuum and should not be affected by the resonator potential. This is likely be due to a tip selective effect associated with the momentum dependence of the tunneling current. Indeed, in the Tersoff and Haman model,[18] the STM current is proportional to the local density of states at the tip apex. Due to the decaying in the vacuum, only the tail of the wave function is experienced by the tip. At the distance z above the surface, the evanescent electron wave at the Fermi energy can be written as

$$\Psi_k(r_\parallel,z)=\phi_{k_\parallel}(r_\parallel)\exp[-\sqrt{\alpha^2+k_\parallel^2}z], \quad (1)$$

where $\phi_{k_\parallel}$ is the in-plane Bloch wave part and α^2 depends on the work function W: $\alpha^2=2\ mW/\hbar^2$. This equation shows that the smaller the $k_\parallel$, the larger the STM current. In other words, small emission angle electrons dominate the tunneling current. This simple result remains valid for every bias voltage.

For the bulk electrons, the confinement between step edges fixes the same $\bar{k}_\parallel$ wave vector than for the surface electrons but the corresponding energy is different due to the different dispersion (energy origin and effective mass). The bulk energy is not only determined by the parallel (in-plane) contribution. As the perpendicular contribution corresponds to the band dispersing in the ΓL direction of the Brillouin zone, the bulk states form a continuum

$$E_B=\frac{\hbar^2\bar{k}_\parallel^2}{2m_B}+E_B(k_z), \quad (2)$$

where $E_B(k_z)$ is the dispersion relation of the bulk band in the ΓL direction. However, according to the Tersoff and Haman model, the tip current is maximum for minimum emission angle and then a peak is expected for the maximum value of k_z i.e., the L high-symmetry point. By using Eq. (2) and the calculated band-structure dispersion along the ΓL direction of Au,[19] it is possible to determine the perpendicular wave vectors involved in the spectral resonance. By taking into account the experimental spectral width and energy position of the confined bulk states, we find that the k_z values are in a small momentum domain close to the L point: $k_z\in[k_L,\Delta k_z]$, with: $\Delta k_z/k_L=0.07$. The energy position of the interference pattern leads us to the conclusion that this perpendicular position correspond to the L point, i.e., the extremum of the first bulk band. Therefore, the bulk states which contribute to the interference pattern in the energy range (−1.1 eV; −0.5 eV) are the bulk band-gap edge states. As a consequence, the momentum distribution of the laterally confined bulk states is found on the free-electron parabola characterized by the bulk effective mass as shown by the dotted line in Fig. 2.

In the last section of this paper, we will show that the bulk states can also be sensitive to the weak potential associated with a surface reconstruction and that its surface part can exhibit an energy-dependent spatial modulation of the electron density for energies close to the energies corresponding to the Brillouin-zone boundaries associated with the reconstruction superperiodicity. In a recent paper[12] on electronic properties of the vicinal Au(23 23 21) surface, we demonstrated by angle-resolved photoemission spectroscopy that the surface electrons experience the surface reconstruction. This reconstruction similar to the well-known herringbone reconstruction of Au(111) (Ref. 20) is associated with periodic fcc and hcp domains separated by stacking faults. Due to the vicinality, the threefold symmetry of the Au(111) is broken and only one domain orientation is present leading to a superperiodicity along the step edges. Bragg diffraction corresponding to this surface superperiodicity leads to the formation of several gaps in the surface band structure at the corresponding Brillouin-zone boundary. These minigaps have been evidenced by angle-resolved photoemission spectroscopy and scanning tunneling spectroscopy. This Bragg mechanism is revealed in STS measurements by the spatial modulation of the surface electron density, in particular the π dephasing through the gaps. This is illustrated in Fig. 3(b) where we report a differential conductance map representing the dI/dV signal for different energies and along a line in the middle of the terrace (about two reconstruction supercells). This dI/dV map illustrates the variation of the electronic density in energy and position. A constant current line scan [Fig. 3(b)] shows that the hcp region appears slightly higher than the fcc one and both domains are lower than the ridges as observed in the herringbone reconstruction of Au(111). It was interpreted as an electronic effect due to a weakly attractive potential in the hcp regions compared to the fcc ones.[21,22] The spectroscopic map illustrates the variation of the local density in energy. In Fig. 3(a), we report an angle-resolved photoemission map in the direction parallel to step edges. It exhibits the dispersion of the surface state above −0.435 eV (the two dashed lines representing the two spin-orbit bands) and the bulk band-gap edge (illustrated by the dotted line). Slightly above the energy of the surface state

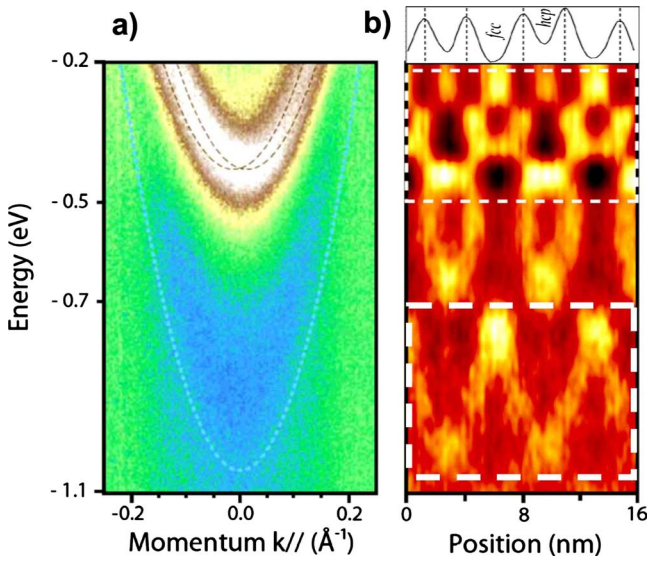

FIG. 3. (Color online) (a) Band structure close to the $\bar{\Gamma}$ point of the surface Brillouin zone (measured by angle resolved photoemission spectroscopy (ARPES)). Upper and lower dashed lines correspond, respectively, to the spin-orbit splitted Shockley state and the projected bulk gap edge. (b) STM topographic profile along a line in the middle of a terrace and parallel to step edges and dI/dV map (I_t=0.5 nA and U_g=−1.1 V) along this line. Dashed rectangles in the right part of the figure highlight the similar dephasing behavior of the surface (top) and bulk (down) states.

onset (E_S=−0.435 eV), Fig. 3(a) shows that the electron density is mainly located in the ridges and hcp domains corresponding to low potential regions. A sudden dephasing appears near E=−410 meV and E=−310 meV, the lower and upper gap energies as expected in the nearly free-electron model.[12] Between the energy of the bulk gap edge at $\bar{\Gamma}$(E=−1.05 eV) and the onset of the surface state (E_S=−0.435 eV), some electron densities with a spatial modulation and a complex energy dependence are clearly visible. Like in the case of the perpendicular direction of steps, this modulation can only result from the bulk states. Surprisingly, the bulk electron density exhibits dephasing behaviors which are reminiscent to those discussed above for the surface state. This is illustrated by the two dashed rectangles of Fig. 3(b). However, we would like to point out that the bulk modulation is expended in the energy scale as shown by the size of the involved energy range, between −0.45 and −0.2 eV for the surface states and −1.05 and 0.7 eV for the bulk states. This dilatation is a direct consequence of the relative surface and bulk effective masses which lead to a more pronounced dispersion for bulk states. This spectral behavior indicates that the surface part of the bulk states is also affected by Bragg scattering associated with the surface reconstruction. The existence of a well-defined density modulation, which only involves the parallel components of the momentum, strongly suggests that its perpendicular component (k_z) is fixed. From the energy position, we can deduce that this perpendicular component can be identified with the L point of the bulk Brillouin zone. In the energy range between −0.7 eV and the onset of the surface state band, the spectral modulation seems to reproduce that observed between −1.05 and −0.7 eV. This replicate can be explained by the existence of the confined states between the steps. Indeed, we expect exactly the same density modulation in the parallel direction for each step induced quantum well state. Therefore, a series of replicates shifted in energy of the spectral signature of the quantum well ground state should be observed. However, as the STS data have been recorded along a line in the middle of the terrace, only perpendicularly confined states having a finite weight in the middle of the terrace can contribute. As shown in Fig. 2(a), the odd confined modes exhibit a negligible weight in the middle of the terrace and do not contribute to modulation of the density of states reported in Fig. 3(b). Therefore, in the energy range below the surface state, only the fundamental and the second excited modes should contribute to the spectral modulations, at −1.05 eV for the ground state and −0.7 eV for the excited state. This energy difference of 0.35 eV is in good agreement with the difference of the corresponding quantum well (QW) states deduced from Fig. 2 (ΔE=0.38 eV when renormalized by the bulk-surface effective-mass ratio). The observed density modulation of the bulk states has likely the same origin than the surface states density modulation. It reflects the surface superperiodicity and results from a two-dimensional (2D) Bragg scattering. This suggests that the bulk states, or more precisely their surface parts, exhibit a periodicity which is not simply the periodicity of the bulk lattice but also the superperiodicity of the surface. However, some differences should exist between the two kinds of states. Indeed, the superperiodicity potential induces minigaps in the surface state band whereas it only affects the surface part of the bulk states. Evidently, it does not induce an energy gap in the bulk band structure but affects the spatial distribution of the electron density at the surface as measured by STS.

In this paper, we show three different examples of electronic interference patterns due to scattering of bulk states by nanostructures or nanostructurated surfaces. We have observed the confinement of bulk states in quantum corrals, in terraces of a vicinal surface, and also the density modulation due a reconstruction-induced superperiodicity. Therefore, the bulk states reproduce the behavior of surface states. This is possible to measure because the component of the wave vector normal to the surface is fixed in the states imaged by STS. The bulk states contributing to the STS signal correspond to the edge of the surface-projected bulk band so that the corresponding perpendicular component of the wave vector can be identified with the L point of the Brillouin zone corresponding to the extremum in the bulk band structure in the ΓL direction.

*Corresponding author; malterre@lpm.u-nancy.fr

[1] J. Friedel, Nuovo Cimento **7**, 287 (1958).
[2] M. F. Crommie, C. P. Lutz, and D. M. Eigler, Nature (London) **363**, 524 (1993).
[3] Y. Hasegawa and Ph. Avouris, Phys. Rev. Lett. **71**, 1071 (1993).
[4] P. T. Sprunger, L. Petersen, E. W. Plummer, E. Lægsgaard, and F. Besenbacher, Science **275**, 1764 (1997).
[5] M. Ternes, C. Weber, M. Pivetta, F. Patthey, J. P. Pelz, T. Giamarchi, F. Mila, and W. D. Schneider, Phys. Rev. Lett. **93**, 146805 (2004).
[6] L. Bürgi, O. Jeandupeux, H. Brune, and K. Kern, Phys. Rev. Lett. **82**, 4516 (1999).
[7] M. F. Crommie, C. P. Lutz, and D. M. Eigler, Science **262**, 218 (1993).
[8] J. Li, W. D. Schneider, R. Berndt, and S. Crampin, Phys. Rev. Lett. **80**, 3332 (1998).
[9] H. Jensen, J. Kröger, R. Berndt, and S. Crampin, Phys. Rev. B **71**, 155417 (2005).
[10] C. Tournier-Colletta, B. Kierren, Y. Fagot-Revurat, and D. Malterre, Phys. Rev. Lett. **104**, 016802 (2010).
[11] A. Mugarza, A. Mascaraque, V. Pérez-Dieste, V. Repain, S. Rousset, F. J. García de Abajo, and J. E. Ortega, Phys. Rev. Lett. **87**, 107601 (2001); A. Mugarza and J. E. Ortega, J. Phys.: Condens. Matter **15**, S3281 (2003).
[12] C. Didiot, Y. Fagot-Revurat, S. Pons, B. Kierren, C. Chatelain, and D. Malterre, Phys. Rev. B **74**, 081404(R) (2006).
[13] C. Didiot, A. Tejeda, Y. Fagot-Revurat, V. Repain, B. Kierren, S. Rousset, and D. Malterre, Phys. Rev. B **76**, 081404(R) (2007); C. Didiot, S. Pons, B. Kierren, Y. Fagot-Revurat, and D. Malterre, Nat. Nanotechnol. **2**, 617 (2007).
[14] L. Petersen, P. Laitenberger, E. Lægsgaard, and F. Besenbacher, Phys. Rev. B **58**, 7361 (1998).
[15] J. I. Pascual, A. Dick, M. Hansmann, H.-P. Rust, J. Neugebauer, and K. Horn, Phys. Rev. Lett. **96**, 046801 (2006).
[16] B. V. Andryushechkin, K. N. Eltsov, and V. M. Shevlyuga, Surf. Sci. **472**, 80 (2001).
[17] L. Bürgi, O. Jeandupeux, A. Hirstein, H. Brune, and K. Kern, Phys. Rev. Lett. **81**, 5370 (1998).
[18] J. Tersoff and D. R. Hamann, Phys. Rev. B **31**, 805 (1985).
[19] C. B. Sommers and H. Amar, Phys. Rev. **188**, 1117 (1969).
[20] J. V. Barth, H. Brune, G. Ertl, and R. J. Behm, Phys. Rev. B **42**, 9307 (1990).
[21] W. Chen, V. Madhavan, T. Jamneala, and M. F. Crommie, Phys. Rev. Lett. **80**, 1469 (1998).
[22] L. Bürgi, H. Brune, and K. Kern, Phys. Rev. Lett. **89**, 176801 (2002).